J inst

Published by IOP Publishing for Sissa Medialab

Received: *January 7, 2020*
Accepted: *March 5, 2020*
Published: *April 14, 2020*

15th Topical Seminar on Innovative Particle and Radiation Detectors
14–17 October 2019
Siena, Italy

2020 JINST 15 C04028

JUNO detector: design and construction

P. Lombardi on behalf of the JUNO Collaboration

[a]*Istituto Nazionale di Fisica Nucleare,*
Via Celoria 16, 20133 Milano, Italy

E-mail: paolo.lombardi@mi.infn.it

Abstract: The Jiangmen Underground Neutrino Observatory (JUNO) is a 20-kton multi-purpose liquid scintillator detector currently being built in a dedicated underground laboratory located in the Jiangmen province (Southern China). JUNO' s main physics goal is the determination of the neutrino mass ordering using electron anti-neutrinos from two nuclear power plants at a baseline of about 53 km. This crucial measurement is supported by an unprecedented energy resolution of 3% at 1 MeV. Furthermore, the detector could observe supernova neutrinos, study atmospheric, solar and geo-neutrinos and perform exotic searches. Several challenges have been overcome during the construction of the largest liquid scintillator detector in the world, such as compatibility of the sphere material, mechanics of the stainless steel structure, scintillator light yield and transparency, PMTs detection efficiency. In this talk, JUNO's design as well as the status of its construction will be presented, together with a short excursion into its rich R&D program.

Keywords: Large detector systems for particle and astroparticle physics; Neutrino detectors; Liquid detectors; Scintillators, scintillation and light emission processes (solid, gas and liquid scintillators)

https://doi.org/10.1088/1748-0221/15/04/C04028

Contents

1 Introduction

The Jiangmen Underground Neutrino Observatory (JUNO) [1] is a 20 kton liquid scintillator detector currently under construction near Kaiping, Jiangmen city, Guangdong province. The JUNO site is at a distance of 53 km from both Yangjiang and Taishan Nuclear Power Plants (NPPs) in order to maximize sensitivity for mass ordering determination that is the primary goal of the experiment [1]. The thermal power of both the NPPs are expected to be 26.6 GWth at the end of 2020. The total overburden of the underground experimental hall is about 700 m.

The JUNO detector will play a central role also in the measurements of the oscillation parameters $\sin^2\theta_{12}$, Δm^2_{12} and $|\Delta m^2_{ee}|$, as well as of the atmospheric squared mass difference Δm^2_{31} with sub percentage precision. Numerous additional physics measurements are expected [1], like solar neutrinos, geoneutrinos, supernova neutrinos, leptonic CP-violating phase and proton decay. Last but not least, the Taishan Antineutrino Observatory (TAO) will be built and operated next to the Taishan power plant ($\sim$ 30 m) to reduce systematic effects in the reactor antineutrino spectrum measured by JUNO. Physics of mass ordering determination will be described in detail in the following paragraph.

1.1 Mass ordering determination

The detection of reactor antineutrinos is based on the Inverse Beta Decay (IBD) of protons occurring on the Liquid Scintillator in the experiment Central Detector, where the electron antineutrino reacts with a proton producing a positron and a neutron according to:

$$\overline{\nu} + \mathrm{p} \rightarrow \mathrm{e}^+ + \mathrm{n} \tag{1.1}$$

2020 JINST 15 C04028

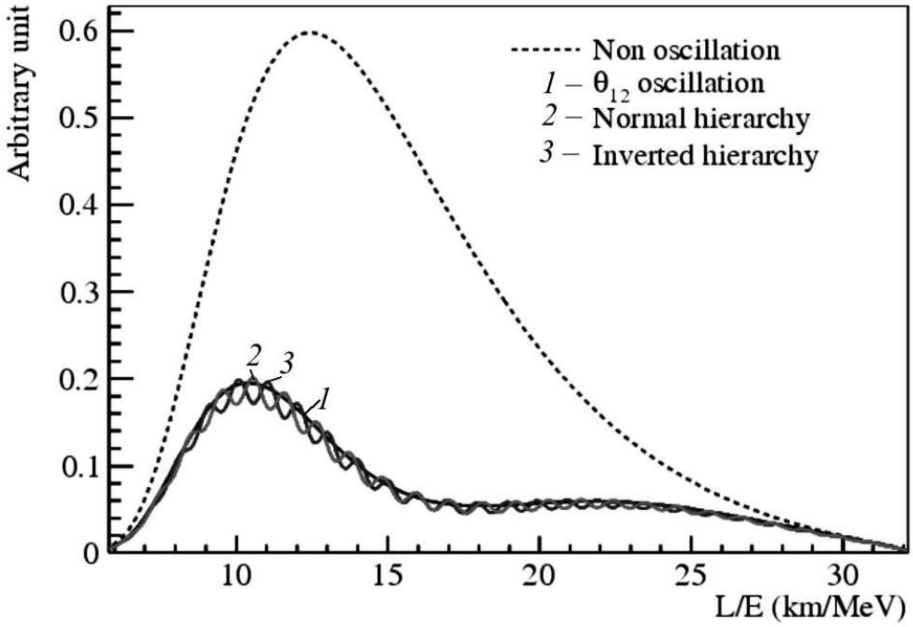

Figure 1. L/E reactor spectrum with effect of P_{ee} electron neutrino survival probability [1].

Since the mass of a neutron is much larger than the mass of a positron, the energy of the positron relates to the energy of the antineutrino.

A very high background rejection is possible due to the nature of the IBD reaction (1.1) since its signature is the coincidence of a prompt and a delayed signal. The prompt signal comes from the energy loss and the subsequent annihilation of the positron. The delayed signal comes from the neutron being captured by hydrogen in the liquid scintillator with a mean capture time of $\sim 200\,\mu$s and the emission of a photon with an energy of 2.2 MeV from the n capture on Hydrogen.

Electron antineutrinos, travelling from the NPP to the JUNO site, undergo a suppression due to flavor oscillation. Through suitable approximations the survival probability $\mathrm{P_{ee}}$ can be written as:

$$P_{\overline{\nu}\mathrm{e}\to\overline{\nu}\mathrm{e}} = 1 - \sin^2 2\theta_{13}(\sin^2\theta_{12}\sin^2\Delta_{32} + \cos^2\theta_{12}\sin^2\Delta_{13}) - \sin^2 2\theta_{12}\cos^4\theta_{13}\sin^2\Delta_{12} \qquad (1.2)$$

with $\Delta_{ij} = (\Delta m^2_{ij}L)/(4E)$ which is shown for both cases of the normal hierarchy and the inverted hierarchy in figure 1. The y axis is proportional to the event rate, while on the x axis the ratio of L/E is reported. The dashed line is the un-oscillated spectrum. The continuous black line is the spectrum distorted and suppressed as an effect of the solar oscillation: this large effect is the key for the very precise determination of the two solar mixing parameters Δm^2_{12} and $\sin^2\theta_{12}$.

The lines marked as 2 and 3 in the figure 1, superimposed on the smooth black line, display the effect of the interference term driven by the atmospheric mass squared difference.

The frequency of the ripple depends on the absolute value of $|\Delta m^2_{31}|$ (which therefore can also be determined with high accuracy by precisely fitting the ripple itself), while its phase depends on the sign, as shown by the reciprocal shift of the 2 and 3 lines in the figure 1.

Unraveling the phase of the ripple is a clue for the mass ordering determination. To this purpose, obviously, the ripples information must be preserved as much as possible throughout the detection process, setting the stringent requirement on the energy resolution of being equal or better than 3%, which represents by far the greatest challenge of the experiment.

The analysis, $\chi 2$-based, will be done by fitting the energy spectrum with the expected spectra both for the normal and inverted mass ordering. The results will determine the neutrino mass ordering with a sensitivity $\Delta\chi^2$. The obtained sensitivity will depend both on the acquired amount of statistics and the energy resolution.

If we consider 6 years of data acquisition with 26.6 GWth reactor power, corresponding to about 100,000 IBD events, and the design energy resolution of $3\%\sqrt{E(\mathrm{MeV})}$ in a 20 kton fiducial volume, the reachable sensitivity is expected to be 3–4σ, corresponding to 9–16$\Delta\chi^2$.

2 The JUNO detector structure

2.1 The central detector

The JUNO design is based on a spherical unsegmented liquid scintillator detector that will push such a technology beyond the present limit, as far as the mass (20 kton) and the energy resolution (3%) are concerned, see figure 2. Starting the description from the center of the detector, the 20 kton of liquid scintillator are contained in a 35.4 m diameter acrylic sphere composed by 265 pieces of 120 mm thick spherical panels. The net weight of the acrylic sphere is about 600 tons. The acrylic sphere is surrounded by a stainless steel truss with a diameter of about 40.1 m, which will perform the twofold task to sustain the vessel, by relieving its internal stress, and to provide the anchor

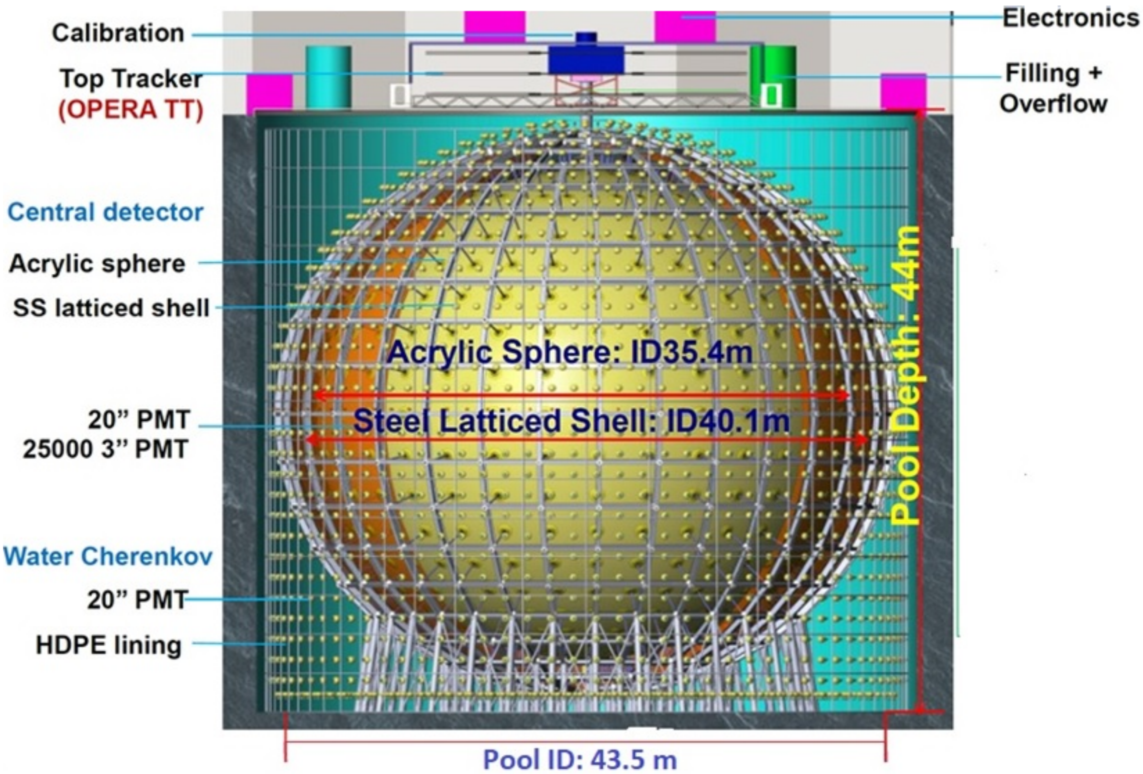

Figure 2. Schematic view of the JUNO detector.

support for Photo-Multiplier Tubes (PMTs) immersed in a high purity water pool. Two sizes of PMTs will be used in JUNO, namely 20.000 20 inch PMTs and 25.000 3 inch PMTs. Compensating electromagnetic coils are wrapped in circular rings around the stainless steel truss in two directions to ensure a proper shielding against the Earth's magnetic field.

2.2 The veto detector

In order to reduce the experimental background, the central detector will be submerged into a huge ($\sim$ 43.5 m) cylindrically shaped water pool in a deep underground hall. The water pool, equipped with 2.400 20 inch PMTs, will contain 40 kton of ultra-pure water to provide shielding from the radioactivity of the surrounding rock and the PMT glass. Therefore, instrumented water pool provide a very efficient active Cherenkov detector to tag crossing muons [2]. The JUNO veto detector includes also a Top Tracker detector placed on top of the water pool. It was a part of the former OPERA detector [3, 4] in Gran Sasso Laboratory. The recovered plastic scintillator will be arranged in three layers with a spatial resolution of $2.6 \times 2.6\,\mathrm{cm}^2$ and a coverage of approximately 60% of the surface of the top of the pool. Together, the Cherenkov detector and the Target Tracker enable one to track cosmogenic muons providing the foundation for a partial volume muon veto.

2.3 Photomultiplier tubes

Due to the demanding energy resolution required by the experiment, one of the key components is the photon detection system to maximize the collection of the scintillation light created by the interactions of the neutrinos with liquid scintillator. The light detection system will comprise about 20.000 20 inch and 25.000 3 inch PMTs placed at 1.8 m from the sphere. The 20 inch PMTs inventory consists of 5.000 dynode PMTs (R12860HQE) produced by *Hamamatsu Photonics K.K.*, while the remaining PMTs are Micro Channel Plate PMTs manufactured by the Chinese company *North Night Vision Technology Co. Ltd.* (NNVT). The total photocathode coverage of the detector will be around 78%, a high value considering the implication of detector dimension and shape in terms of money, technological challenge and number of channels.

Delivered PMTs are stored in Zhongshan Pan-Asia in southern of China, where the performance testing systems are installed and running since July 2017 [5]. Two container test systems with electromagnetic shielding and commercial electronics were designed for mass acceptance tests. As a second testing system, two scanning stations are set up to calibrate the photon detection efficiency from 168 point-like light sources.

The PMTs from the two companies are similar in performances, and it is worth mentioning that the PMT's detection efficiency (quantum efficiency $\times$ collection efficiency) has reached a value close to 30% [6].

The testing results show that the NNVT PMTs have lower after pulse probability and lower radioactive background, while the Hamamatsu PMTs have lower transit time spread giving better space reconstruction. Additionally, 25.000 3 inch PMTs, which contribute 2.5% photocathode coverage, are also deployed to serve as an additional standalone calorimetry with virtually no saturation and better energy scale linearity since they are expected to work almost always at the Single Photon-Electron regime. All the 3 inch PMTs are supplied by *Hainan Zhanchuang Company (HZC)*.

2020 JINST 15 C04028

Waterproof potting was carefully studied and a potting procedure was finally developed and certified for reliability by means of accelerating ageing tests both in pressure and temperature.

Furthermore, in order to prevent chain reaction caused by single PMT imploding, an acrylic protective cover has been carefully designed and tested in several implosion test done in a large vessel at 0.6 Mpa water pressure. The acrylic protection cover will be placed on the top of each 20 inch PMT with steel cover mounted on the bottom as supporting structure.

2.4 Electronics

The JUNO electronics is composed by two systems: the front-end and the back-end electronics. The front-end is located in an underwater box very close to the PMTs in order to minimize the length of cables and maximize the signal to noise ratio. Each box collects, using custom made underwater feed-through connectors, the analog signals from three neighboring PMTs. Signals are digitized in the Global Control Unit, a custom Field Programmable Gate Array board with 3 ADU and 3 HV units. The digital signal and trigger information are forwarded to the dry electronics by means of up to 100 m long CAT5 Ethernet cables.

The back-end electronics [7] is instead located outside the water pool and includes the DAQ and the trigger. In this system, back-end cards are used as concentrators to collect and compensate the incoming trigger request signals. An FPGA mezzanine card handles all trigger request signals. The signals from the various back-end cards are sent to 21 RMU (Reorganize & Multiplex Unit) cards, and their sum is forwarded to the Central Trigger Unit. The main challenge of the whole electronics system is the very strict criteria on reliability: less than 0.5% failure rate over 6 years for the PMTs full readout chain.

2.5 The calibration system

The knowledge of the detector energy resolution and of the energy scale non-linearity, is one of the key point of the experiment. The energy response depends on the detector geometry and the optical properties of the relevant detector components (scintillator, photomultipliers, electronics, acrylic sphere, etc.). In order to achieve an energy scale uncertainty better than 1%, an efficient calibration system is of great importance. The calibration system will consist of four complementary subsystems [8]:

1. ACU — Automated Calibration Unit. The ACU is a one dimensional system and can be operated along the vertical axis adjusting the rope length with a spool drive system. The frequency will be weekly and the accuracy a few mm.

2. CLS — Cable Loop System. The CLS is a two dimensional system and can be operated to scan the vertical planes adjusting the rope length with a spool drive system. The frequency will be monthly and the accuracy a few cm.

3. GTCS — Guide Tube Calibration System. The GTCS is also a two dimensional system and can be operated to scan the outer surface of the detector adjusting the rope length with a spool drive system. The frequency will be weekly and the accuracy a few cm.

2020 JINST 15 C04028

4. ROV — Remotely Operated Vehicle. The ROV is a three dimensional system and can move freely within the detector to fully scan the whole detector. The frequency will be seasonally or annually and the accuracy around 4 cm.

Three kinds of radiation sources, including neutron sources (^{241}Am-^{9}Be, ^{241}Am-^{13}C, ^{241}Pu-^{13}C, ^{252}Cf), positron sources (^{22}Na, ^{68}Ge, ^{40}K, ^{90}Sr) and γ sources (^{40}K, ^{54}Mn, ^{60}Co, ^{137}Cs), will be used for calibration.

2.6 Liquid scintillator

The JUNO Liquid Scintillator is an organic compound containing molecules featuring benzene rings that can be excited by ionizing particles; it consists of Linear Alkyl Benzene (LAB) as solvent, doped with 2,5-Diphenyloxazole (PPO 2.5 g/l) as primary solute, and 1,4-Bis(2-methylstyryl)benzene (bis-MSB 3 mg/l) as wavelength shifter.

Low-background conditions are crucial for the success of JUNO. From the point of view of the liquid scintillator, this means that the concentration of radioactive impurities inside the mixture should result in an activity of the same level or below the rate of neutrino events.

Radio-purity levels are usually specified by the concentration of ^{232}Th, ^{238}U and ^{40}K in the scintillator. The baseline scenario, which will be desirable for the detection of reactor antineutrinos in JUNO, assumes a contamination in the range of 10^{-15} g/g of U and Th and 10^{-15} g/g of ^{40}K in the scintillator.

A more stringent regime, in the realm of 10^{-17} g/g, would instead be needed to accomplish the JUNO neutrino Astroparticle program [1].

Moreover, the JUNO physics program requires reaching an energy resolution (3% at 1 MeV) never achieved before in any large-mass liquid scintillator neutrino experiment. In order to reach the necessary light collection, the attenuation length of the scintillator has to be comparable to the diameter of the acrylic chamber (above 20 m for a wavelength of 430 nm).

In order to achieve these stringent requirements on the scintillator optical and radioactive purity, a composite system has been developed, see figure 3. This system makes use of the technologies developed for LAB and other scintillators in the frame of high-mass neutrino experiments such as Borexino [9], KamLAND [10], SNO+. The first two plants, Alumina oxide column and vacuum distillation column will be deployed overground in a dedicated building.

They will refine the raw LAB mainly removing optical contaminants through absorption mechanism and heaviest impurities (mainly ^{238}U, ^{232}Th and ^{40}K) through vacuum distillation [11].

A mixing PPO/Bis-MSB plant will provide purified solute through water extraction. The scintillator cocktail will be finally sent underground through a 1.3 km long pipe to the final purification system that includes the water extraction plant and steam stripping plant.

All the four plants are very demanding in terms of performances (high purification factor), cleanliness (MIL STD 1246 Level 50), tightness (10^{-8} mbar-l/s) and flow rate (6000 kg/h). In order to prove and qualify the purification process on a LAB based liquid scintillator, it has been decided to build pilot plants with all the complexity, feature and functions of the JUNO plants but with a scaled reduced flow rate of 100 kg/h. These pilot plants have been installed and operated at Daya Bay underground laboratory from beginning of 2017 to end of 2018 on one of the Daya Bay detector.

2020 JINST 15 C04028

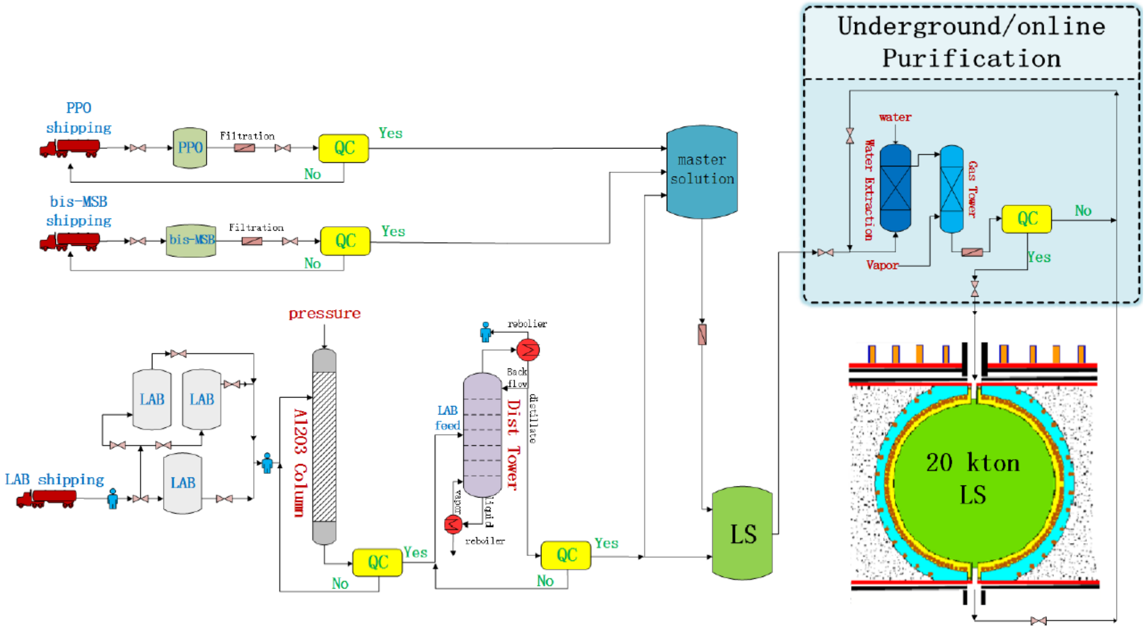

Figure 3. Schematic view of the JUNO scintillator purification system.

Several tests have been done to carefully study the optical and radio purity performances of the purification system and the preliminary results are very promising.

2.7 The Online scintillator internal radioactivity investigation system: OSIRIS

The OSIRIS system [12], a low background ancillary JUNO detector facility, will be installed underground close to the JUNO scintillator purification plants. Its main goal will be to prove the radio-purity quality of the scintillator reached during the commissioning of the purification system and to ensure flawless operation by continuously monitoring the radio-purity during the detector filling. OSIRIS is composed by an acrylic cylinder filled with liquid scintillator, with a dimension of 3 m in diameter and 3 m in height, placed in the center of a cylindrical water tank of 10 m diameter and 11 m height. The vessel will be instrumented with 81 PMTs (20 inch) to detect the scintillation light. The external tank, filled with ultra-pure water, will also be equipped with 12 PMTs (20 inch) to behave as a water Cherenkov veto detector in order to reduce the background from crossing muons and rocks and PMTs radioactivity. The system dimensions are optimized to reach a sensitivity to the baseline radio-purity of 10^{-16} g/g for U/Th within 1 day measurement for $\sim$ 19 tons liquid scintillator.

2.8 The Taishan Antineutrino Observatory: TAO

In the frame of the JUNO mass ordering measurement, it is mandatory a precise estimation of the unoscillated reactor antineutrino spectrum to eliminate the possible model dependence of the JUNO mass ordering determination. The existing model for the energy-dependent reactor flux is subject, however, to both the anomalous bump observed in reactor antineutrino spectra at 5 MeV and a fine structure yet unknown [13].

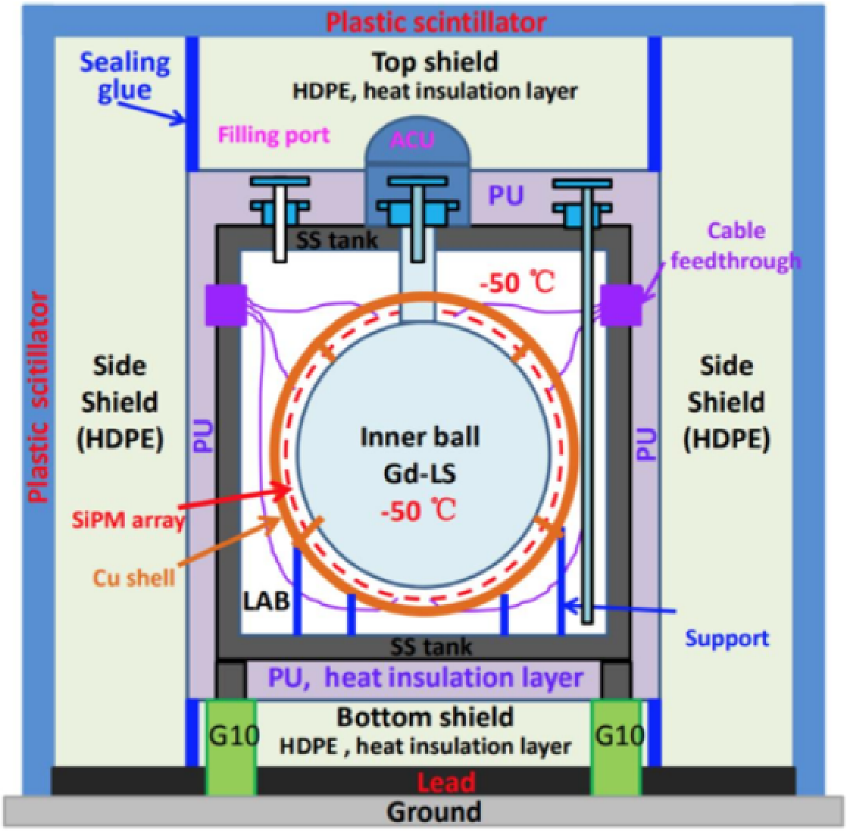

Figure 4. Schematic view of the TAO detector.

To accomplish this measurement, a dedicated detector has been developed: the Taishan Antineutrino Observatory (TAO). The TAO apparatus will be installed at a distance of 30 m from the 4.6 GWth-power core of one of the Taishan nuclear power plants. The detector consists of an acrylic sphere, filled with several tons of gadolinium loaded scintillator submerged in pure LAB, see figure 4. The gadolinium is used for its high cross section in neutron capture. Antineutrinos will be revealed via the IBD reaction in the scintillator and the light emitted will be detected by the surrounding Silicon Photomultipliers (SiPM) featuring a photo-electron detection efficiency of $\sim$ 50% considering a perfect coverage and a light yield of 4500 photoelectrons at an energy of 1 MeV. The expected energy resolution will be better than $3\%\sqrt{E(\mathrm{MeV})}$ [14]. The scintillator will be operated at -50 degree Celsius to reduce the SiPM noise.

3 JUNO progress and schedule

The JUNO underground laboratory excavation started in January 2015. So far, the slope tunnel (1265 m) and the vertical shaft (563 m) have been fully excavated. The former will allow porting the scintillator underground, the latter will enable access of personnel and construction materials. The excavation is now progressing with the digging of the main experimental hall while most of the auxiliary hall and service tunnels have been already digged.

The civil construction is foreseen to be fully completed by about the middle of 2020. The preparation and production of the detector components, e.g. phototubes, acrylic panels, etc., has already started in 2016, while the global onsite installation will be completed by the fall of 2021. This scenario is in line to ensure the completion of the scintillator fill and the startup of data taking at the beginning of 2022.

Acknowledgments

The author wishes to thank the organizers for the invitation to contribute to such an interesting and enlightening conference.

References

[1] JUNO collaboration, *Neutrino Physics with JUNO*, *J. Phys.* **G 43** (2016) 030401 [arXiv:1507.05613].

[2] R.G. Wang et al., *Water Cherenkov Detector of the JUNO Veto System*, talk presented at the *European Physical Society Conference on High Energy Physics*, Heidelberg, Germany, 4–9 June 2018.

[3] T. Adam et al., *The OPERA experiment target tracker*, *Nucl. Instrum. Meth.* **A 577** (2007) 523 [physics/0701153].

[4] R. Acquafredda et al., *The OPERA experiment in the CERN to Gran Sasso neutrino beam*, 2009 *JINST* **4** P04018.

[5] JUNO collaboration, *Large photocathode 20-inch PMT testing methods for the JUNO experiment*, 2017 *JINST* **12** C06017 [arXiv:1705.05012].

[6] H. Zhang, Z. Wang, F. Luo, A. Yang, Z.-H. Qin, C. Yang et al., *Study on relative collection efficiency of PMTs with spotlight*, *Radiat. Detect. Technol. Meth.* **3** (2019) 20.

[7] B. Clerbaux, *The JUNO experiment and its electronics readout system*, talk presented at the *EPS-HEP Conference 2019*, Gent, Belgium, 10–17 July 2019.

[8] Q.M. Zhang et al., *JUNO Central Detector and its Calibration System*, in proceedings of the *38th International Conference on High Energy Physics*, Chicago, U.S.A., 3–10 August 2016, PoS(ICHEP2016)967.

[9] Borexino collaboration, *The Borexino detector at the Laboratori Nazionali del Gran Sasso*, *Nucl. Instrum. Meth.* **A 600** (2009) 568 [arXiv:0806.2400].

[10] KamLAND collaboration, *Precision Measurement of Neutrino Oscillation Parameters with KamLAND*, *Phys. Rev. Lett.* **100** (2008) 221803 [arXiv:0801.4589].

[11] P. Lombardi et al., *Distillation and stripping pilot plants for the JUNO neutrino detector: Design, operations and reliability*, *Nucl. Instrum. Meth.* **A 925** (2019) 6 [arXiv:1902.05288].

[12] H. Steiger, *OSIRIS: Status of the Detector Hardware Development*, https://indico.cern.ch/event/738555/contributions/3174135/attachments/1736380/2808991/OSIRIS_HardwareFinland18.pdf.

[13] D.V. Forero, R. Hawkins and P. Huber, *The benefits of a near detector for JUNO*, arXiv:1710.07378.

[14] J. Cao, *Measuring High Resolution Reactor Neutrino Spectrum with JUNO-TAO*, talk presented at the Technical Meeting on Nuclear Data for Anti-neutrino Spectra and Their Applications, IAEA, Vienna, Austria, 23-26 April 2019.

2020 JINST 15 C04028